High-order optical harmonic generation from solid surfaces

Article *in* Applied Physics B · October 1996

DOI: 10.1007/s003400050115

CITATIONS
113

READS
78

2 authors:

Dietrich von der Linde
University of Duisburg-Essen
332 PUBLICATIONS **15,503** CITATIONS

SEE PROFILE

Kazimierz Rzazewski
Polish Academy of Sciences
229 PUBLICATIONS **5,899** CITATIONS

SEE PROFILE

Appl. Phys. B 63, 499–506 (1996)

Applied Physics B Lasers and Optics

High-order optical harmonic generation from solid surfaces

D. von der Linde[1], **K. Rzàzewski**[2]

[1] Institut für Laser- und Plasmaphysik, Universität Essen, D-45117 Essen, Germany
[2] Center for Theoretical Physics and College of Science, Al. Lotników 32/46, P-02-668 Warsaw, Poland

Received: 1 July 1996

Abstract. During the interaction of an intense ultrashort laser pulse with solid targets, a thin layer of surface plasma is generated in which the density drops to the vacuum level in a distance much shorter than the wavelength. This sharp plasma–vacuum boundary performs an oscillatory motion in response to the electromagnetic forces of the intense laser light. It is shown that the generation of reflected harmonics can be interpreted as a phase modulation experienced by the light upon reflection from the oscillating boundary. The modulation side-bands of the reflected frequency spectrum correspond to odd and even harmonics of the laser frequency. Retardation effects lead to a strong anharmonicity for high velocities of the plasma–vacuum boundary. As a result, harmonic generation is strongly enhanced in the relativistic regime of laser intensities.

PACS: 42.65.Ky; 52.40.Nk; 52.50.Jm

The generation of optical harmonics of very high order [1] is one example of the many interesting new phenomena that occur when extremely intense ultrashort laser pulses interact with matter. The production of odd harmonics exceeding the hundredth order was observed in noble gases [2]. This type of harmonic generation has been studied extensively and is now fairly well-understood. The basic physical mechanism of harmonic generation in gases is the highly nonlinear electronic response of the atoms to the strong electric field of the laser pulse.

More than a decade ago a different type of high-order harmonic generation was observed when nanosecond pulses from a CO_2 laser interacted with solid targets [3, 4]. In this case both odd and even harmonic orders occurred, indicating that the harmonic radiation was produced under physical conditions lacking inversion symmetry. Theoretical models developed by Bezzerides et al. [5] and Grebogi et al. [6] proposed that harmonic generation is due to the strong anharmonicity of the electron motion across a steep density gradient of the surface plasma produced by the laser pulse. These models assumed that an abrupt, almost step-like discontinuity of the density developed in the expanding plasma due to ponderomotive forces of the laser light counterbalancing the expansion. A characteristic high-frequency cut-off in the harmonic spectra was predicted, which was in agreement with the experimental observations. According to these models the cut-off frequency is given by the plasma frequency corresponding to the upper level of the density profile.

Progress in the generation of extremely intense ultrashort laser pulses has led to new interest in harmonic generation from solid targets. During the interaction of an intense ultrashort pulse with the surface of a solid, the time for plasma expansion is limited. A thin surface layer of plasma is developed in which the electron density drops from a value corresponding to solid density to vacuum in a distance much shorter than the wavelength of light. Thus ultrafast laser–solid interaction naturally provides a plasma with an extremely steep density gradient. One expects the production of odd and even harmonics resulting from the anharmonicity of the electronic motion at the plasma–vacuum interface. High-order harmonic generation from solid targets has recently been observed experimentally using femtosecond [7, 8] and picosecond [9] laser pulses.

Generation of harmonics of low order from plasmas can be treated by perturbation theory [10, 11]. However, it is clear that perturbative methods are inadequate for the treatment of laser–plasma interaction at very high intensities. In a recent theoretical investigation of high-order harmonic generation from a plasma–vacuum boundary detailed computer simulations were used [12]. Although computer simulations provide a very useful information, large amounts of computer time are necessary to perform the calculations, and it is often difficult to gain some basic physical insight from the numerical data only. The gap was filled by the recent work of Lichters et al. [13], who used relativistic cold plasma fluid equations to interpret the results of their particle-in-cell simulations.

Dedicated to Prof. F. P. Schäfer on the occasion of his 65th birthday.

They showed that the detailed simulations are in excellent agreement with a simple model in which harmonic generation is interpreted as a reflection from an oscillating mirror surface treated in full relativistic representation.

In this paper, we discuss high-order harmonic generation from a plasma–vacuum boundary in terms of the oscillating mirror model [13, 14]. In Sect. 1 the oscillating mirror model is introduced. Section 2 gives a qualitative discussion of the electromagnetic driving forces. From this discussion the polarization selection rules for odd and even harmonics can be derived in a straightforward manner. Formulas for the harmonic spectra are given in Sects. 3 and 4. In Sect. 5, we discuss the oscillation amplitude and show that the interference between the incident and the reflected wave are expected to play an important role.

1 The oscillating mirror model

Let us assume a light wave of frequency ω_0 and wave vector k_0 impinging from vacuum on some supercritical plasma. Assume further that the plasma density is constant in the half-space $z < 0$ and drops to vacuum for $z > 0$ over a very short distance. A large portion of the light is back-reflected at the critical density surface. In the supercritical region, the wave is evanescent and decays in a short length given by the skin depth.

The interaction with light generates some periodic motion of the plasma in response to the electromagnetic forces. It is assumed that the duration of the light pulse is sufficiently short so that the motion of the ions may be neglected. The ions are treated as a fixed positive background charge. We are interested in the modulation of the reflected wave caused by the periodic changes of the electron density.

The electromagnetic forces push and pull electrons back and forth across the boundary. The basic approximation of the oscillating mirror model [13, 14] is to neglect the details of the changes of the electron density profile and to represent the collective electronic motion by the motion of the boundary of the supercritical region. This boundary represents an *effective reflecting surface* performing an oscillatory motion, the oscillating mirror.

Neglecting for a moment retardation effects the phase shift of the reflected wave resulting from a sinusoidal displacement of the reflecting surface in the z-direction, $s(t) = s_0 \sin \omega_m t$, is given by

$$\phi(t) = (2\omega_0 s_0 / c) \cos\theta \sin \omega_m t , \tag{1}$$

where θ is the angle of incidence, ω_m the modulation frequency, and s_0 the amplitude. The electric field of the reflected wave is given by

$$E_R \propto e^{-i\omega_0 t} e^{i\phi(t)} = e^{-i\omega_0 t} \sum_{n=-\infty}^{n=\infty} J_n(\chi) e^{-in\omega_m t} , \tag{2}$$

where $J_n(\chi)$ is the Bessel function of order n and

$$\chi = (2\omega_0 s_0 / c) \cos\theta . \tag{3}$$

Here we have made use of the well-known Jacobi expansion:

$$e^{-iz\sin\omega_m t} = \sum_{n=-\infty}^{n=\infty} J_n(\chi) e^{-in\omega_m t} . \tag{4}$$

The phase modulation produced by the oscillating mirror gives rise to a series of sidebands at distances from the carrier frequency ω_0 given by multiples of the modulation frequency ω_m.

It will be shown in the following that the reflecting surface performs a periodic motion at a frequency $2\omega_0$, or a superposition of ω_0 and $2\omega_0$, depending on the polarization and angle of incidence of the incoming light. Thus, the modulation frequencies provided by the mirror motion are $\omega_m = \omega_0$ and/or $\omega_m = 2\omega_0$. The key point is that this type of modulation produces sidebands representing even and odd harmonics of the fundamental frequency ω_0. These ideas suggests an interpretation of high-order harmonic generation from a plasma–vacuum interface as a phase modulation from a periodically moving reflecting surface (Doppler shift).

For modulation at a very high frequencies (corresponding to optical frequencies) relativistic retardation effects come into play which lead to important modifications of (2). The generalization of (2) properly including retardation effects will be discussed in Sect. 3.

2 Driving forces

To gain some qualitative insight into what type of motion is performed when the reflecting surface is driven by the electromagnetic forces, let us consider the classical orbit of an electron in a linearly polarized plane wave of frequency ω_0. It is well-known that during one fundamental cycle of the field the electron performs a "figure-eight-motion" in a plane spanned by the electric field vector and the wave vector [15]. Figure 1 illustrates the situation. Note that there is a longitudinal component of the excursion (parallel to the wave vector) oscillating at $2\omega_0$, and a transverse component (parallel to the electric field) oscillating at ω_0. Recall that for weak fields the longitudinal component is small and the transverse part dominates. The condition of a weak field is given by $a_0 \ll 1$, where a_0 is the relativistic parameter:

$$a_0 = \frac{eA_0}{mc^2} . \tag{5}$$

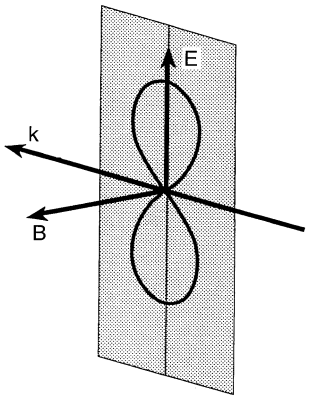

Fig. 1. Figure-eight-orbit of a free electron in a linearly polarized plane wave of wave vector **k**. **E** and **B** denote, respectively, the electric and the magnetiic field vector

Here A_0 is the amplitude of the vector potential of the incident wave in the Coulomb gauge, and mc^2 is the electron rest energy.

We shall now make the assumption that the collective motion of the electrons near the plasma–vacuum interface is qualitatively similar to the figure-eight-motion of a single electron. It is then possible to draw some conclusions concerning the frequency of the periodic motion of the reflecting surface for different polarizations and angles of incidence and to predict the type of harmonic radiation expected under these conditions:

(i) *p-polarized light*: The electric and the magnetic field are, respectively, parallel and perpendicular to the plane of incidence. The electrons move in the plane of incidence. The electron boundary is driven at frequencies ω_0 and $2\omega_0$, because both the transverse and the longitudinal component of the electron velocity contribute to the motion of the boundary. It follows that in this case both *even* and *odd* harmonics with p-polarization are generated.

(ii) *s-polarized light*: The electric field is parallel to the plasma–vacuum interface. The electrons move in a plane perpendicular to the plane of incidence. In this configuration only the longitudinal component contributes, while the transverse component of the electron motion is ineffective. The normal motion of the mirror is driven at one frequency only, $\omega_m = 2\omega_0$. It follows that the reflected light is composed of s-polarized *odd* harmonics. There are no s-polarized even harmonics.

In addition to the harmonics discussed so far there is harmonic generation from the oscillating mirror which cannot be interpreted as phase modulated reflected light. This type of harmonic emission follows from a consideration of the changes of the electrical charge density at the plasma–vacuum interface induced by the electromagnetic forces. Forward or backward motion of the reflecting surface leads to a surplus or a deficiency of electrons in the boundary region. Since the ions are considered as immobile, an electric dipole sheet is formed at the plasma–vacuum boundary. For oblique incidence there is a periodic variation of the electric dipole moment along the direction with a spatial frequency given by the parallel component of the wave vector of the incident light. Figure 2 illustrates this situation. The charge distribution is somewhat similar to the charge distribution associated with a surface plasmon wave.

Let us consider oblique incidence of s-polarized fundamental light. In this case the dipole sheet is driven at $2\omega_0$. It follows immediately that the dipole sheet radiates p-polarized second harmonic in the specular direction. When the plasma–vacuum boundary is driven sufficiently hard *p-polarized* high-order *even* harmonics are generated.

Summarizing the qualitative discussion, some basic selection rules of high-order harmonic generation from surfaces can be formulated (Table 1). For oblique incidence of p-polarized fundamental light p-polarized even and odd harmonics are obtained. For s-polarized incident light the situation is more complicated. For oblique incidence we have even harmonics with p-polarization and odd harmonics with s-polarization. Only odd harmonics

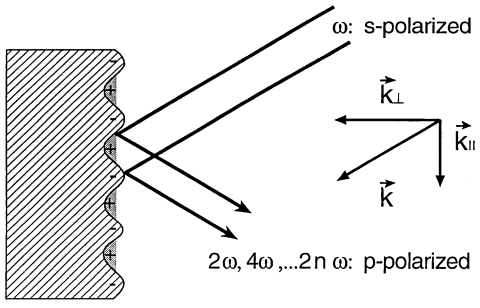

Fig. 2. Charge distribution at the plasma–vacuum boundary. The plus-signs signify the constant positive background charge due to the fixed ions. The minus-signs represent the negative charge due to electrons pushed back and forth across the boundary

Table 1. Polarization selection rules

	s-pol. harmonics	p-pol. harmonics
s-pol. fundamental	odd	even
p-pol. fundamental	forbidden	odd & even

are expected for normal incidence. A rigorous derivation of these polarization selection rules was first given by Lichters et al. [13].

It is interesting to point out that for the lowest-order reflected harmonics the polarization selection rules obtained from the oscillating mirror model are in agreement with results of perturbation theory [11, 12]. Only p-polarized (second and third) harmonics are produced by p-polarized fundamental light, whereas s-polarized light produces p-polarized second harmonic and s-polarized third harmonic.

3 Reflection of light from a moving mirror

We shall now calculate the frequency spectrum of a monochromatic light wave reflected from a surface performing a sinusoidal motion. Let us choose the x- and z-direction parallel and normal to the surface, respectively, and let θ be the angle of incidence of the light in the x–z-plane. Assume further s-polarized incident light with the electric vector perpendicular to the x–z-plane. The electric field can be written:

$$E(t, x, z) = E_0 \exp(-\mathrm{i}\omega_0(t - x/c \sin\theta - z/c \cos\theta)). \quad (6)$$

The excursion of the surface along the z-direction is given by

$$s(t, x) = s_0 \sin(\omega_m \xi) = s_0 \sin(\omega_m(t - x/c \sin\theta)). \quad (7)$$

Equation (7) takes into account that for oblique incidence the periodic variation of the electromagnetic forces along the x-direction produces a periodic surface deformation. The periodicity is determined by the parallel component of the wave vector, $k_x = \omega_0/c \sin\theta$.

The maximum surface amplitude s_0 is limited by the condition that the velocity must not exceed the speed of

light, $s_0 < c/\omega_m$. For s-polarization, we have $\omega_m = 2\omega_0$, as explained above, and this condition implies $\chi < \cos\theta$.

We assume that the reflected wave can be written in the general form of a plane wave propagating in the specular direction:

$$E_R = G(u) = G(t - x/c\sin\theta + z/c\cos\theta). \tag{8}$$

At this point in the discussion of the oscillating mirror model the actual value of the reflection coefficient is of minor importance. However, for an estimate of the total electromagnetic forces acting on the boundary, the phase shifts of the reflected fields are quite important, as will be shown in Sect. 5. Here, we assume for simplicity that the surface is totally reflecting. The function $G(u)$ then is obtained from the condition that the total electric field must vanish on the reflecting surface, i.e. for $z = s(t, x)$:

$$E_R(t, x, s(t, x)) + E(t, x, s(t, x)) = 0. \tag{9}$$

Both sides of (9) are only functions of the variable $\xi = t - x/c\sin\theta$. Although the functional form of $E(t, x, z)$ as given by (6) represents a monochromatic wave it follows from the explicit time dependence of the expressions in (9) that the reflected field is not monochromatic. To obtain the frequency spectrum of the reflected wave the Fourier transform of $G(u)$ must be calculated,

$$\tilde{G}(\omega) = \int_{-\infty}^{\infty} \exp(i\omega u) G(u)\,du, \tag{10}$$

where

$$u = \xi - s_0/c\cos\theta\sin(\omega_m\xi). \tag{11}$$

With a transformation of variable using (11) the Fourier transform can readily be performed. The result is

$$\tilde{G}(\omega) = -2\pi E_0 \sum_{n=-\infty}^{n=\infty} \frac{1}{1 + n\omega_m/2\omega_0} \times J_n((1 + n\omega_m/2\omega_0)\chi)\delta(\omega - \omega_0 - n\omega_m), \tag{12}$$

where J_n are the Bessel functions of order n. The frequency spectrum depends only on the parameter χ given by (3). Note that (12) reduces to a form equivalent of (2) for low modulation frequencies, $\omega_m \ll \omega_0$.

For a s-polarized fundamental wave we have $\omega_m = 2\omega_0$, and the spectrum of the reflected wave has odd harmonic components. The spectral intensity distribution of the harmonics can be written:

$$S((2n + 1)\omega_0) = (\pi E_0)^2 \left(\frac{J_n((n + 1)\chi)}{(n + 1)} - \frac{J_{n+1}(n\chi)}{n} \right)^2, \tag{13a}$$

where n is an arbitrary integer.

Harmonic generation by a p-polarized incident wave can be treated in a similar way. In this case, the *magnetic* field is perpendicular to the x–z-plane, and the electric field in (6), (8) and (9) must be replaced by the magnetic field. Some caution is required for large surface excursions, when the local surface normal deviates from the global surface normal. This effect is neglected here. As explained in the previous section, the mirror motion can be described as a superposition of oscillations at two frequencies, $2\omega_0$ and ω_0. The spectrum of the reflected wave contains p-polarized even and odd harmonics. The harmonic spectrum produced by the ω_0 component of the mirror oscillation alone is given by

$$S(n\omega_0) = (\pi E_0)^2 \left(\frac{J_{n-1}(\frac{1}{2}(n + 1)\chi)}{\frac{1}{2}(n + 1)} - \frac{J_{n+1}(\frac{1}{2}(n - 1)\chi)}{\frac{1}{2}(n - 1)} \right)^2. \tag{13b}$$

Examples of calculated harmonic spectra for different values of χ are shown in Fig. 3 for s-polarized incident light, and in Fig. 4 for p-polarized light. Note that the efficiency of high-order harmonic generation increases strongly with χ. According to (13a) the 115th harmonic would be produced with a strength of 10^{-5} in the highly relativistic case $\chi = 0.98$.

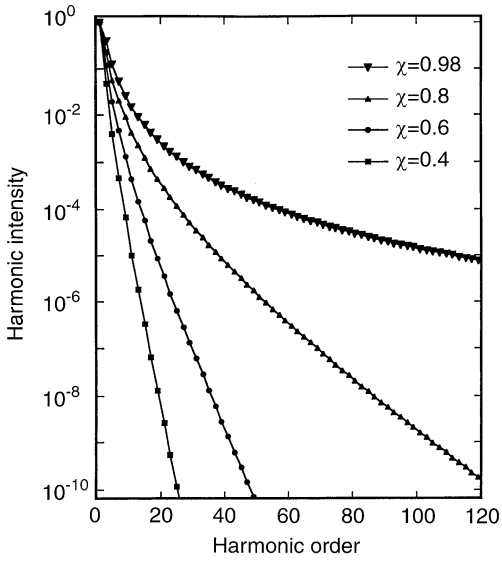

Fig. 3. Spectra of odd harmonics generated by s-polarized light for different values of χ (13a)

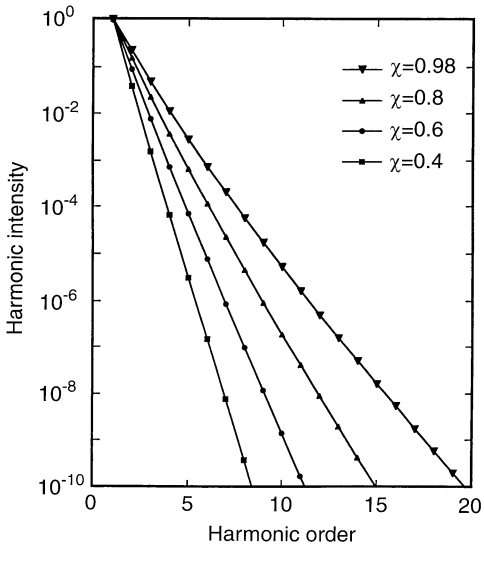

Fig. 4. Spectra of even and odd harmonics generated by p-polarized light for different values of χ (13b)

Comparison of Figs. 3 and 4 indicates that for the same value of χ, the high-frequency roll-off of the harmonic spectra produced by p-polarized light is much faster than the roll-off for s-polarized light. The formal explanation of this effect is the following. The roll-off is determined by the fast decrease of the Bessel functions with increasing order. Because the modulation frequency for s- and p-polarized light differ by a factor of two ($2\omega_0$ and ω_0), the order of the Bessel functions representing a given harmonic frequency is about a factor of two higher in the case of p-polarization as compared with s-polarization. Compare, for example, the production of the 11th harmonic by s- and p-polarized light. In the first case, the 11th harmonic is obtained from (13a) with $n = 5$, whereas in the second case the 11th-harmonic order requires $n = 11$ in (13b). However, it will be shown later that higher values of χ in the argument of the Bessel functions strongly counteract this apparent disadvantage of p-polarization.

4 Harmonic radiation from surface charges

An interesting particularly of the selection rules predicted by the model is that a fundamental wave with s-polarization produces *s-polarized odd* and *p-polarized even* harmonics. The latter cannot be interpreted in terms of a phase-modulated reflected wave, because there is no incident light with p-polarization. To obtain the spectrum of the p-polarized even harmonics we must explicitly consider the radiation from the induced surface dipoles. The key point is that retardation effects come into play when the excursion of the reflecting surface gets large at very high light intensity. Under these conditions the surface dipole sheet radiates a spectrum of high-order even harmonics.

The charge density and the electric current normal to the surface can be written as

$$\rho(z,t)/\rho_0 = \Theta(s_0 \sin(2\omega_0(t - x/c\sin\theta)) - z) - \Theta(-z); \tag{14}$$

$$j_z(t,x,z)/\rho_0 = 2\omega_0 s_0 \cos(2\omega_0(t - x/c\sin\theta)) \times \Theta(s_0 \sin(2\omega_0(t - x/c\sin\theta)) - z). \tag{15}$$

$\Theta(z)$ denotes the Heaviside step function. The fields may be calculated from the retarded potentials. The tedious, but straightforward calculation is outlined in the Appendix. The result shows that the p-polarized electric field is composed of even harmonics, as expected from the qualitative discussion in Sect. 2. The harmonic spectrum is given by

$$S(2n\omega_0) = \frac{4\pi\rho_0^2 c^2}{\omega_0^2} \frac{\tan^2\theta}{\cos^4\theta} \left(\frac{J_n(n\chi)}{n}\right)^2. \tag{16}$$

It is interesting to note that, apart from the prefactors, the functional form of (16) is the same as (13a) and (13b).

5 Oscillation amplitude

The examples of harmonic spectra shown in Figs. 3 and 4 indicate that the number of harmonic orders exceeding a given value increases with χ. According to (3) χ is proportional to the oscillation amplitude s_0 of the reflecting surface. It is therefore interesting to make an estimate of s_0 under various conditions.

From physical considerations, we expect that the maximum surface excursion produced by the effective external driving force is limited by the restoring force of the plasma. The latter is given by $m\omega_p^2$, where m is the mass of the electron and ω_p the plasma frequency. The static force balance is adequate for low driving frequencies, $\omega \ll \omega_p$. To estimate the dynamic oscillation amplitude s in nonrelativistic limit the equation of a driven harmonic oscillator can be used:

$$\frac{d^2}{dt^2} s + \omega_p^2 s = \frac{e}{m} F_{em}. \tag{16}$$

The oscillation amplitude at the frequency ω is then given by

$$s(\omega) = \frac{eF_{em}(\omega)}{m(\omega_p^2 - \omega^2)}, \tag{17}$$

where F_{em} is the electromagnetic force. The effective driving force at the plasma–vacuum boundary is given by the normal component of the total electromagnetic force resulting from the interference of the fields of the incident and the reflected wave.

Let us first consider the case of s-polarization. In this case the electric field vector is parallel to the surface. The motion in the normal direction is driven by the magnetic force. In the lowest-order approximation the equation of motion can be written:

$$\frac{d^2}{dt^2} s + \omega_p^2 s = \frac{e}{mc} v_y B_x; \tag{18}$$

$$\frac{d}{dt} v_y = \frac{e}{m} E_y.$$

The Fourier amplitude of the surface motion at 2ω is then given by

$$s(2\omega) = \frac{i}{(\omega_p^2 - 4\omega^2)\omega} \frac{e^2}{2m^2 c} E_y(\omega) B_y(\omega). \tag{19}$$

The Fourier amplitudes $E_y(\omega)$ and $B_y(\omega)$ of the total electric and magnetic field at the plasma–vacuum boundary can be calculated from the Fresnel formulas using the dielectric function of the plasma in the form

$$\varepsilon(\omega) = 1 - \frac{\omega_p^2}{\omega^2}. \tag{20}$$

In the limit $\omega \ll \omega_p$, the final result for the oscillation amplitude s_0 can be cast in the form

$$\frac{s_0}{\lambda} = \frac{1}{2\pi} \frac{\omega^2}{\omega_p^2} a_0^2 (\cos\theta \sin\delta_s) = \frac{1}{2\pi} \frac{\omega^2}{\omega_p^2} a_0^2 F_s(\theta), \tag{21}$$

where λ is the fundamental wavelength, and δ_s is the phase angle of the Fresnel complex coefficient of reflection for s-polarization, $r_s = |r_s| e^{i\delta_s}$. $F_s(\theta)$ represents the dependence of s_0/λ on the angle of incidence θ. Note that the phase angle δ_s is implicitly dependent on θ.

For normal incidence we have $\sin\delta_s \approx \delta_s \approx 2\omega/\omega_p$, and (21) takes the form [13]

$$\frac{s_0}{\lambda} = \frac{1}{\pi}\frac{\omega^3}{\omega_p^3}\, a_0^2 . \tag{22}$$

An inspection of the fields at the boundary reveals that in this configuration there is a node of the electric field close to the boundary, as a result of *destructive interference* of the incident and the reflected wave. The electric field amplitude is reduced to a value of $2E_0\omega/\omega_p$, where E_0 is the amplitude of the incident electric field. This leads to the additional factor ω/ω_p in (22). Note that (22) represents the maximum value of the surface amplitude, because for s-polarization s_0/λ decreases monotonically with the angle of incidence.

For p-polarization both the electric and the magnetic force contribute to the normal motion of the surface. The amplitude of motion at the frequency 2ω caused by the *magnetic force* can be obtained from (21) simply by replacing δ_s with δ_p, where δ_p is the phase angle of the complex coefficient of reflection for p-polarization, $r_p = |r_p|e^{i\delta_p}$:

$$\frac{s_0}{\lambda} = \frac{1}{2\pi}\frac{\omega^2}{\omega_p^2}\, a_0^2(\cos\theta\sin\delta_p) = \frac{1}{2\pi}\frac{\omega^2}{\omega_p^2}\, a_0^2 F_p(\theta) . \tag{23}$$

The response of the surface to the *electric force* is quite interesting. The effective driving force is the normal component of the total electric field at the boundary. Inserting the corresponding force term into (16) leads to the following expression for the normalized surface amplitude s_0/λ in the limit $\omega \ll \omega_p$:

$$\frac{s_0}{\lambda} = \frac{1}{2\pi}\frac{\omega^2}{\omega_p^2}\, a_0(2\sin\theta\cos(\delta_p/2)) = \frac{1}{2\pi}\frac{\omega^2}{\omega_p^2}\, a_0 G_p(\theta) . \tag{24}$$

Let us compare (21) and (23), representing magnetic driving, with (24), representing electric driving. In the non-relativistic limit $a_0 < 1$ the surface amplitude produced by electric driving is larger, being proportional to a_0, whereas in the magnetic case the surface amplitude varies with a_0^2. More importantly, however, it can be shown that *constructive interference* of the electric fields of the incident and the reflected wave is possible in p-polarization. The driving electric field is enhanced by constructive interference and reaches values close to $2E_0$ at large angles of incidence.

The functions $F_s(\theta)$, $F_p(\theta)$, and $G_p(\theta)$ on the r.h.s. of (21), (23), and (24) describe the angular dependence of s_0/λ. According to (13a), (13b) and (16), the overall angular dependence of harmonic generation is determined by $\chi = 4\pi\cos\theta\ s_0/\lambda$, which involves an additional factor $\cos\theta$. The angular functions including this term are plotted vs θ in Fig. 5. The plot provides a direct comparison of the angular dependence of harmonic generation for p- and s-polarized fundamental light. It can be seen that a maximum value of ≈ 1 is obtained for an angle of incidence $\theta \approx 45^\circ$ in the case of electric driving by p-polarized light (solid line). Note that for magnetic driving the values of the angular functions are much smaller, both in p-polarization (dashed line) and s-polarization (dotted line). The maximum value of about 0.2 occurs at normal incidence.

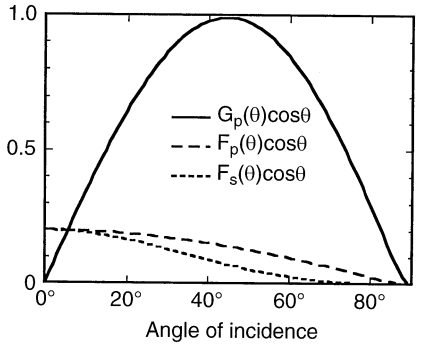

Fig. 5. Angular dependence of χ for p-polarized light and electric driving (*solid line*), and magnetic driving (*dashed line*). The *dotted line* is the angular dependence for s-polarized light

6 Summary

The theory of the interaction of very intense laser radiation with plasmas is a field of great complexity. Theoretical investigations of laser–plasma interaction often end in detailed numerical simulations which assume the character of computer experiments. This is also true for earlier treatments of high-order harmonic generation from overdense plasmas. There is clearly a need to develop simple physical models which describe the essential physics and provide some physical understanding.

We have discussed harmonic generation from a plasma–vacuum boundary in terms of a phase modulation of light upon reflection from a periodically moving surface. Generation of odd and even harmonics and polarization selection rules can be derived from this oscillating mirror model in a straightforward manner. The results are in agreement with lowest-order perturbation theory and also with rigorous analytical models and numerical simulations [13] of high-order harmonic generation.

Making the assumption of a sinusoidal mirror oscillation, simple analytical expressions for different types of harmonic spectra were obtained. The oscillation amplitude s_0 was estimated from the balance of the plasma restoring force and the electromagnetic driving forces in the non-relativistic limit. Efficient harmonic generation requires large values of s_0/λ. The ultimate limit is given by the restriction that the velocities of the particles must not exceed the speed of light, i.e. $s_0/\lambda < 1/(4\pi)$ for a driving frequency $\omega_m = 2\omega$.

It was shown that the principal determinants of the motional amplitude of the surface are:

(i) The relativistic field parameter a_0;
(ii) The frequency ratio ω/ω_p;
(iii) The interference between the incident and the reflected wave.

The last point concerns the partial constructive or destructive interference of the field components at the boundary. Interference reduces or enhances electromagnetic forces with respect to the forces of the incident wave depending on the phase shift suffered by the reflected wave.

The expressions for s_0/λ indicate that efficient high-order harmonic generation requires values of the relativistic field parameters a_0 of the order of unity, which

corresponds to laser intensities $I\lambda^2 \approx 10^{18}\,\mathrm{W/cm^2\,\mu m^2}$. The efficiency of high-order harmonic generation reaches a maximum in the highly relativistic regime $a_0 \gg 1$, when the oscillation amplitude s_0/λ approaches the ultimate relativistic limit.

The frequency factor ω/ω_p signifies the resistance of the medium to perturbations of the electronic charge density. One is led to the conclusion that solid density plasmas are not the optimum choice for harmonic generation. For typical solid densities and optical frequencies we have $\omega/\omega_p \approx 10$, indicative of very strong plasma restoring forces. From the consideration of the frequency factor it appears that a slightly overdense plasma is preferable in high-order harmonic generation [13]. Furthermore, in a plasma of lower density a considerable enhancement of the oscillation amplitude is expected to occur for resonant excitation, when the driving frequency equals the plasma frequency. This effect was demonstrated by Lichters et al. [13] for magnetic driving of a step-like density profile, where the resonance condition is $\omega/\omega_p = 2$. It should also be kept in mind that in typical experimental situations it will be difficult to maintain a step-like density discontinuity during the interaction with the laser pulse. More likely, one is dealing with a plasma–vacuum boundary having experienced some broadening during the interaction. One would expect that the simple model discussed here ceases to be a good picture of harmonic generation when the plasma–vacuum boundary is spread out over a distance comparable with the electron excursion.

Acknowledgements. This work was supported by the Deutsche Forschungsgemeinschaft and by the European Union under Human Capital and Mobility. The authors are greatly indebted to J. Meyer-ter-Vehn, R. Lichters and A. Pukhov for enlightening discussions on harmonic generation and also for making their manuscript available to us prior to publication. K. R. gratefully acknowledges financial support under KBN Grant 2P03B04209.

Appendix

We start from (14) and compute the scalar potential generated by this charge density using the general formula

$$\boldsymbol{\Phi}(\mathbf{r},t) = \int \mathrm{d}^3\mathbf{r}' \int \mathrm{d}t' \, \frac{\rho(\mathbf{r}',t')}{|\mathbf{r}'-\mathbf{r}|}\,\delta\left(t' + \frac{|\mathbf{r}'-\mathbf{r}|}{c} - t\right). \tag{A1}$$

We first represent the step functions by their Fourier representation, perform the t' integration and expand the resulting exponent into harmonics:

$$\begin{aligned}\boldsymbol{\Phi}(\mathbf{r},t) = \frac{\rho_0}{2\pi\mathrm{i}} \sum_{n\neq 0} \exp(2\omega n\mathrm{i}t) \int \mathrm{d}^3\mathbf{r}' \\ \times \frac{\exp(2\omega n\mathrm{i}(|\mathbf{r}'-\mathbf{r}| - x'\sin\theta)/c}{|\mathbf{r}'-\mathbf{r}|} \\ \times \int_{-\infty}^{+\infty} \mathrm{d}\lambda \, \frac{\mathrm{e}^{-\mathrm{i}\lambda z'}}{\lambda} J_n(s_0\lambda).\end{aligned} \tag{A2}$$

The integration over λ is performed with the help of formula 6.693 from [16],

$$\begin{aligned}\int_{-\infty}^{+\infty} \mathrm{d}\lambda \, \frac{\mathrm{e}^{-\mathrm{i}\lambda z'}}{\lambda} J_n(s_0\lambda) \\ = \frac{(\sqrt{s_0^2 - z'^2} - \mathrm{i}z')^n - (-1)^n(\sqrt{s_0^2 - z'^2} + \mathrm{i}z')^n}{n s_0^n}\end{aligned} \tag{A3}$$

for $|z'| \leq s_0$, and zero otherwise. With the substitution $z' = s_0 \sin\varphi$, $0 \leq \varphi \leq 2\pi$, we obtain

$$\begin{aligned}\boldsymbol{\Phi}(\mathbf{r},t) = \frac{\rho_0 a}{2\pi\mathrm{i}} \sum_{n\neq 0} \frac{\exp(2\omega n\mathrm{i}t)}{n} \int_0^{2\pi} \mathrm{d}\varphi \cos\varphi \mathrm{e}^{-\mathrm{i}n\varphi} \int \mathrm{d}x' \, \mathrm{d}y' \\ \times \frac{\exp(2\omega n\mathrm{i}(|\mathbf{r}'-\mathbf{r}| - x'\sin\theta)/c)}{|\mathbf{r}'-\mathbf{r}|}.\end{aligned} \tag{A4}$$

The potential is independent of y. Shifting the x' integration by x, and using polar coordinates r and ϑ in the x–z-plane we get

$$\begin{aligned}\boldsymbol{\Phi}(\mathbf{r},t) = \frac{\rho_0 a}{2\pi\mathrm{i}} \sum_{n\neq 0} \frac{\exp(2\omega n\mathrm{i}(t - \sin\theta x/c))}{n} \\ \times \int_0^{2\pi} \mathrm{d}\varphi \cos\varphi \mathrm{e}^{-\mathrm{i}n\varphi} \int_0^{\infty} r \, \mathrm{d}r \\ \times \int_0^{\pi} \mathrm{d}\vartheta \, \frac{\exp(2\omega n\mathrm{i}(\sqrt{r^2+u^2} + r\sin\theta\sin\vartheta)/c)}{\sqrt{r^2+u^2}}\end{aligned} \tag{A5}$$

with $u = z + s_0\sin\varphi$. The integration over ϑ leads to Bessel functions, and the substitution $R = (r^2+u^2)^{1/2}/u$ allows to use formula 6.646 from [16] to obtain

$$\begin{aligned}\boldsymbol{\Phi}(\mathbf{r},t) = \frac{\rho_0 s_0 c}{2\omega\cos\theta} \sum_{n\neq 0} \frac{\exp(2\omega n\mathrm{i}\,T)}{n} \\ \times \int_0^{2\pi} \mathrm{d}\varphi \cos\varphi \exp(-\mathrm{i}n(\varphi + \chi\sin\varphi))\end{aligned} \tag{A6}$$

where $T = t - (x\sin\theta + z\cos\theta)/c$, and χ is given by (3).

The remaining integration gives Bessel functions again and we have

$$\begin{aligned}\boldsymbol{\Phi}(\mathbf{r},t) = \frac{\pi\rho_0 c^2}{2\omega\cos\theta} \sum_{n\neq 0} \frac{\exp(2\omega n\mathrm{i}\,T)}{n^2} \\ \times (-1)^n (J_{n+1}(n\chi) + J_{n-1}(n\chi)).\end{aligned} \tag{A7}$$

Equation (A7) can be simplified using the well-known recurrence relations of the Bessel functions. The potential given by (A7) is a scalar wave travelling in the direction of the reflected wave. The gradient of this potential points in the direction of propagation. Its modulus is given by

$$E_\phi = \frac{2\pi\rho_0 c}{\omega\cos^2\theta} \sum_{n=1}^{\infty} \sin(2\omega n T) \frac{(-1)^n}{n} J_n(n\chi). \tag{A8}$$

There is an additional component of the electric field parallel to the z-direction from the vector potential. The total electric field is perpendicular to the direction of propagation. Thus, we have $E = \tan\theta E_\phi$, and the final result for the spectrum of the p-polarized harmonic emission is (16) in Sect. 4.

$$S(n\omega) = \frac{4\pi^2\rho_0^2 c^2}{\omega^2} \frac{\tan^2\theta}{\cos^4\theta} \left(\frac{J_n(n\chi)}{n}\right)^2. \tag{A9}$$

References

1. See, e.g., *Atoms in Intense Fields*, ed. by M. Gavrila (Academic Press, Boston 1992)
2. J.J. Macklin, J.D. Kmetec, C.L. Gordon III: Phys. Rev. Lett. **70**, 766 (1993)
3. R.L. Carman, D.W. Forslund, J.M. Kindel: Phys. Rev. Lett. **46**, 29 (1981)
4. R.L. Carman, C.K. Rhodes, R.F. Benjamin: Phys. Rev. A **24**, 2649 (1981)
5. B. Bezzerides, R.D. Jones, D.W. Forslund: Phys. Rev. Lett. **49**, 202 (1982)
6. C. Grebogi, V.K. Tripathi, H.H. Chen: Phys. Fluids **26**, 1904 (1983)
7. S. Kohlweyer, G.D. Tsakiris, C.G. Wahlström, C. Tillman, I. Mercer: Opt. Comm. **117**, 431 (1995)
8. D. von der Linde, T. Engers, G. Jenke, P. Agostini, G. Grillon, E. Nibbering, A. Mysyrowicz, A. Antonetti: Phys. Rev. A **52**, R25 (1995)
9. P.A. Norreys, M. Zepf, S. Moustaizis, A.P. Fews, J. Zhang, P. Lee, M. Bakarezos, C.N. Danson, A. Dyson, P. Gibbon, P. Loukakos, D. Neely, F.N. Walsh, J.S. Wark, A.E. Ongor: Phys. Rev. Lett. **76**, 1832 (1996)
10. K. Baumgärtel, K. Sauer: Physical Research, Vol. 4, *Topics on Non-Linear Wave-Plasma Interaction* (Akademie-Verlag Berlin, 1987)
11. D. von der Linde, in: *Laser Interactions with Atoms*, *Solids*, *and Plasmas*, ed. by R.M. More (Plenum Publ. Corpor., New York 1994) p. 207
12. P. Gibbon: Phys. Rev. Lett. **76**, 50 (1996)
13. R. Lichters, J. Meyer-ter-Vehn, A. Pukhov: Phys. Plasmas, in print
14. S.V. Bulanov, N.M. Naumova, F. Pegoraro: Phys. Plasmas **1**, 745 (1994)
15. L.D. Landau, I. Lifshitz: *Cours of Theoretical Physics*, Vol. 2, *The classical Theory of Fields* (Pergamon Press, Oxford 1975)
16. I.S. Gradshtein, I.M. Ryzhik: *Table of Integrals*, *Series and Products* (Academic Press, New York 1965)

.